

---

# LEAVE-GROUP-OUT CROSS-VALIDATION FOR LATENT GAUSSIAN MODELS

---

**Zhedong Liu**

Statistics Program, Computer, Electrical and Mathematical Sciences and Engineering Division  
 King Abdullah University of Science and Technology (KAUST)  
 Kingdom of Saudi Arabia, Thuwal 23955-6900  
 zhedong.liu@kaust.edu.sa

**Håvard Rue**

Statistics Program, Computer, Electrical and Mathematical Sciences and Engineering Division  
 King Abdullah University of Science and Technology (KAUST)  
 Kingdom of Saudi Arabia, Thuwal 23955-6900  
 haavard.rue@kaust.edu.sa

October 11, 2022

## ABSTRACT

Evaluating predictive performance is essential after fitting a model and leave-one-out cross-validation is a standard method. However, it is often not informative for a structured model with many possible prediction tasks. As a solution, leave-group-out cross-validation is an extension where the left-out-groups adapt to different prediction tasks. In this paper, we propose an automatic group construction procedure for leave-group-out cross-validation to estimate the predictive performance when the prediction task is not specified. We also propose an efficient approximation of leave-group-out cross-validation for latent Gaussian models. We implement both procedures in the R-INLA software.

*Keywords:* Cross-Validation, Structured Models, Latent Gaussian Models, R-INLA

## 1 Introduction

The predictive performance of a model is required for assessing or comparing different models. Cross-validation (CV) is a common method to estimate the predictive performance of a model by splitting observed data into a training set and a testing set multiple times [1, 2]. A good CV strategy has the relationship between training sets and testing sets similar to the relation between observed data and unobserved data, hence, CV strategies should be designed according to specific prediction tasks. Nevertheless, many practitioners use CV in the form of leave-one-out cross-validation (LOOCV) without considering their prediction tasks. LOOCV leaves a testing point out to train a model and uses the left-out point (testing point) to validate the prediction iteratively. LOOCV mimics the prediction task when a model is unstructured, which assumes each data point, i.e., covariates and response is sampled independently from a joint distribution. For example, in typical classification models with covariates, the prediction task is defined by using covariates to predict the label. When a model is not unstructured, i.e. a structured model, multiple prediction tasks exist. For instance, the prediction task is not uniquely defined in time-series. The prediction could be predicting the response in an independent replicate of the observed time series, forecasting the response in the future of the observed time series, or interpolating a missing value in the observed time series. LOOCV in time-series mimics the interpolation task, which is seldom considered as a prediction. LOOCV is generally over-optimistic about the predictive performance when a model is structured, an issue extensively discussed extensively in [3]. Throughout this paper, we focus on structured models.

The deficiency of naively employing LOOCV has also been noticed by many researchers in practice. Here we highlight some specific studies in the literature.

- In a biomedical study [4], a multi-level model is used for diagnosis. Their data are collected from different subjects, and each subject has some records. Researchers recommend the subject-wise CV when the model is used for a diagnosis of newly recruited subjects. The subject-wise CV uses all the records not from a specific subject to train the model and uses the records from the subject to validate the prediction. LOOCV or record-wise CV is expected to be too optimistic since the information from the same subject is used for prediction.
- In a study from the petroleum industry [5], a time-series model is used for forecasting. Researchers use leave-future-out cross-validation (LFOCV) [6] to evaluate the model's ability to forecast the production of tight oil wells. LFOCV uses the observations that happen before a time point to train a model and exploits the observation at that time point to evaluate the predictive performance. LOOCV will produce an overly optimistic result since we infer the testing points using their future but we can only use the history to forecast future data.
- In a paleogeology study [7], spatial models are used for predicting species assemblages and environmental conditions in an area geographically separated from the observed area. Researchers use  $h$ -block cross-validation (HCV) [8] to estimate the models' predictive performance. In HCV, along with the testing point, observations within  $h$  km of it are omitted from the training set. LOOCV is again not appropriate due to its usage of unavailable information.

CV variants in the studies adapt to different prediction tasks by adjusting the training sets for each testing set. We can also make LOOCV adapt to the prediction tasks by changing the training set for each data point. We call the adapted LOOCV leave-group-out cross-validation (LGOCV) since the adaptations are done by leaving a group of data out from the training sets. The groups are defined to make the prediction task implicitly implied by CV more similar to the desired prediction task.

In some modeling scenarios, we may not have a primary prediction task, but we still want to have an easy-to-use quantity to describe the predictive performance. We can roughly classify prediction tasks into two types, interpolation tasks and extrapolation tasks. In extrapolation tasks, the observed data provide less information to predict the new data. The meaning of the interpolation and the extrapolation varies in different models. Interpolation tasks are exemplified by padding missing values in time series [9, 10] and kriging in geostatistics [11]. Extrapolation tasks are represented by forecasting in a time series model, predicting data on a territory far away from the observations' location in a spatial model, or predicting data measured from an unobserved stratum in a multilevel model. LOOCV often implies an interpolation prediction task, while an extrapolation task is often more important in structured models.

We propose an automatic group construction method for latent Gaussian models (LGMs) [12, 13] to better assist modelers to assess their models. The automatically constructed group consists of data points most informative to predict the testing point. The aim of our automatic LGOCV is to propose a better default criterion than LOOCV for structured models. If a clear prediction task exists, we recommend using LGOCV designed for the prediction task. Otherwise, the proposed automatized LGOCV is a better option because it reveals more extrapolation performance than LOOCV.

The brute-force way to compute CV is straightforward as we only need to fit models on all possible training sets and compute the utility on the corresponding testing set. However, the computational cost of the brute-force way is prohibitive because a single fit of a modern statistical model is costly. LOOCV requires  $n$  model fits, where  $n$  is the number of observed data points. Thus several methods are proposed to compute CV efficiently for different models: [12] approximates LOOCV by correcting the approximated posterior marginal distributions; [14] computes LOOCV using Pareto-smoothed importance sampling (PSIS). For Gaussian linear regression, closed-form solutions of LOOCV are well-known. Also, many approximation methods were proposed to compute variants of CV similar to LGOCV for specific models [6, 15, 16]. We make LGOCV computationally feasible by deriving an efficient and accurate approximation of LGOCV for LGMs. The automatic group construction procedure and the approximation of LGOCV are implemented efficiently in the R-INLA software[12].

The plan for the paper is as follows. Section 2 contains preliminaries on Bayesian cross-validation and LGMs. Section 3 explains the automatic group construction. Section 4 discusses the approximation of LGOCV. Section 5 compares the approximated LGOCV with the exact LGOCV computed by Markov chain Monte Carlo (MCMC) and demonstrates its use in some real data applications. We end with a general discussion in Section 6.

## 2 Preliminaries

### 2.1 Bayesian Cross-Validation

In the Bayesian framework, if we fit a model on a data set  $\mathbf{y}$ , we will obtain a posterior distribution  $\pi(\boldsymbol{\phi}|\mathbf{y})$ , where  $\boldsymbol{\phi}$  are the model parameters. Bayesian prediction relies on a predictive distribution

$$\pi(\tilde{Y}|\mathbf{y}) = \int \pi(\tilde{Y}|\boldsymbol{\phi}, \mathbf{y}) \pi(\boldsymbol{\phi}|\mathbf{y}) d\boldsymbol{\phi},$$

where  $\tilde{Y}$  is an unobserved data point, and the form of  $\pi(\tilde{Y}|\boldsymbol{\phi}, \mathbf{y})$  is determined by the prediction task.  $\pi(\tilde{Y}|\mathbf{y})$  is validated by external knowledge on  $\tilde{Y}$ , for example, a hypothetical generating process of  $\tilde{Y}$  or actually observed  $\tilde{Y}$ . If a future observation,  $\tilde{y}$ , is observed,  $\pi(\tilde{Y}|\mathbf{y})$  can be validated against  $\tilde{y}$  using a utility function or a loss function. A typical utility function is  $u(\tilde{y}, \mathbf{y}) = \log \pi(Y = \tilde{y}|\mathbf{y})$ .

The idea of LOOCV is using the pair  $(y_i, \mathbf{y}_{-i})$  as a surrogate of  $(\tilde{y}, \mathbf{y})$ , where  $y_i$  is the testing point, and  $\mathbf{y}_{-i}$  is the training set. To make the testing point and the training set a better proxy of the new data and the observed data, leave-group-out cross-validation (LGOCV) uses the pair  $(y_i, \mathbf{y}_{-I_i})$  as a surrogate of  $(\tilde{y}, \mathbf{y})$  instead, where  $I_i$  is an index set containing indices of data removed from the training set. The purpose of  $I_i$  is to make  $(\tilde{y}, \mathbf{y})$  and  $(y_i, \mathbf{y}_{-I_i})$  more similar given a prediction task.

With LGOCV, the mean log predictive density is

$$U_{\text{LGOCV}} = \frac{1}{n} \sum_{i=1}^n \log \pi(Y_i = y_i | \mathbf{y}_{-I_i}), \quad (1)$$

and the mean square error is

$$L_{\text{LGOCV}} = \frac{1}{n} \sum_{i=1}^n (E[Y_i | \mathbf{y}_{-I_i}] - y_i)^2. \quad (2)$$

We can also use different aggregation methods and utility (loss) functions [17, 18] to validate predictions.  $I_i$  can be modified to make LGOCV identical to many variants of CV, including subject-wise CV in [4], LFOCV in [5, 6], HCV in [7, 8], and LOOCV.

### 2.2 Latent Gaussian Models

In this section, we briefly introduce Latent Gaussian Models and its inference using integrated nested Laplace approximation (INLA) [12, 19, 13, 20] to help the readers follow the coming sections. The LGMs can be formulated by

$$\begin{aligned} y_i | \eta_i, \boldsymbol{\theta} &\sim \pi(y_i | \eta_i, \boldsymbol{\theta}), \\ \boldsymbol{\eta} &= \mathbf{A}\mathbf{f}, \\ \mathbf{f} | \boldsymbol{\theta} &\sim N(0, \mathbf{P}_f(\boldsymbol{\theta})), \\ \boldsymbol{\theta} &\sim \pi(\boldsymbol{\theta}). \end{aligned} \quad (3)$$

In LGMs, each  $y_i$  is independent conditioning on its corresponding linear predictor  $\eta_i$  and hyperparameters  $\boldsymbol{\theta}$ ;  $\boldsymbol{\eta}$  is a linear combination of  $\mathbf{f}$ , which is assigned with a Gaussian prior with zero mean and a precision matrix parameterized by  $\boldsymbol{\theta}$ ;  $\mathbf{A}$  is the design matrix mapping  $\mathbf{f}$  to  $\boldsymbol{\eta}$ ;  $\pi(\boldsymbol{\theta})$  is a prior density of hyperparameters.

The model is quite general because  $\mathbf{f}$  can be a combination of many modeling components, including linear model, spatial components, temporal components, spline components, etc. It is also common with linear constraints on the latent effects  $\mathbf{f}$  [21].

We can approximate  $\pi(\mathbf{f}|\boldsymbol{\theta}, \mathbf{y})$  and  $\pi(\boldsymbol{\theta}|\mathbf{y})$  at some configurations,  $\boldsymbol{\theta}_1 \dots \boldsymbol{\theta}_k$ , using INLA. The configurations are located around the mode of  $\pi(\boldsymbol{\theta}|\mathbf{y})$ , denoted by  $\boldsymbol{\theta}^*$ , for numerical integration. Approximations of  $\pi(\boldsymbol{\eta}|\boldsymbol{\theta}, \mathbf{y})$  are computed using the linear relation,  $\boldsymbol{\eta} = \mathbf{A}\mathbf{f}$ . The Gaussian approximation of  $\pi(\mathbf{f}|\boldsymbol{\theta}, \mathbf{y})$  plays an essential role, which is outlined as follows.

We have  $\pi(\mathbf{f}|\boldsymbol{\theta}, \mathbf{y})$  for a given  $\boldsymbol{\theta}$ ,

$$\pi(\mathbf{f}|\boldsymbol{\theta}, \mathbf{y}) \propto \exp \left\{ -\frac{1}{2} \mathbf{f}^T \mathbf{P}_f(\boldsymbol{\theta}) \mathbf{f} + \sum_{i=1}^n \log(\pi(y_i | \eta_i, \boldsymbol{\theta})) \right\}, \quad (4)$$

whose mode is  $\mu_f(\boldsymbol{\theta}, \mathbf{y})$ . The Gaussian approximation of  $\pi(\mathbf{f}|\boldsymbol{\theta}, \mathbf{y})$  is

$$\pi_G(\mathbf{f}|\boldsymbol{\theta}, \mathbf{y}) \propto \exp \left\{ -\frac{1}{2} \mathbf{f}^T (\mathbf{P}_f(\boldsymbol{\theta}) + \mathbf{A}^T \mathbf{C}(\boldsymbol{\theta}, \mathbf{y}) \mathbf{A}) \mathbf{f} + \mathbf{A}^T \mathbf{b}(\boldsymbol{\theta}, \mathbf{y}) \mathbf{f} \right\}. \quad (5)$$

In (5),  $b_i(\boldsymbol{\theta}, \mathbf{y}) = g'_i(\eta_i^*) - g''_i(\eta_i^*)\eta_i^*$ , and  $\mathbf{C}$  is a diagonal matrix with  $C_{ii}(\boldsymbol{\theta}, \mathbf{y}) = -g''_i(\eta_i^*)$ , where  $g_i(\eta_i) = \log(\pi(y_i|\eta_i, \boldsymbol{\theta}))$  and  $\eta_i^* = \mathbf{A}_i \boldsymbol{\mu}_f(\boldsymbol{\theta}, \mathbf{y})$  with  $\mathbf{A}_i$  being  $i$ th row of  $\mathbf{A}$ . The Gaussian approximation is denoted by,

$$\mathbf{f}|\mathbf{y}, \boldsymbol{\theta} \sim N(\boldsymbol{\mu}_f(\boldsymbol{\theta}, \mathbf{y}), \mathbf{Q}_f(\boldsymbol{\theta}, \mathbf{y})), \quad (6)$$

where  $\boldsymbol{\mu}_f(\boldsymbol{\theta}, \mathbf{y}) = \mathbf{Q}_f(\boldsymbol{\theta}, \mathbf{y})^{-1} \mathbf{A}^T \mathbf{b}(\boldsymbol{\theta}, \mathbf{y})$  and  $\mathbf{Q}_f(\boldsymbol{\theta}, \mathbf{y}) = \mathbf{P}_f(\boldsymbol{\theta}) + \mathbf{A}^T \mathbf{C}(\boldsymbol{\theta}, \mathbf{y}) \mathbf{A}$  are the approximated posterior mean and precision matrix of  $\mathbf{f}$  given  $\boldsymbol{\theta}$ . The mean of Gaussian approximation,  $\boldsymbol{\mu}_f(\boldsymbol{\theta}, \mathbf{y})$ , can be further improved using low rank variational Bayes using method in [20].

### 3 Automatic Group Construction

The purpose of our automatic construction is to make the testing points less dependent on the corresponding training sets such that the LGOCV mimics an extrapolation task, in which the unobserved data is often assumed less dependent on the observed data.

In LGMs, the dependency of data is specified by the dependency of linear predictors in (3). The linear predictors are designed to have a Gaussian prior and approximated to be Gaussian in posterior given  $\boldsymbol{\theta}$ , therefore we can use the correlation matrix of  $\boldsymbol{\eta}$  to represent dependency. For fixed  $\boldsymbol{\theta}$ , we have correlation matrices derived from  $\mathbf{P}_f(\boldsymbol{\theta})$  and  $\mathbf{Q}_f(\boldsymbol{\theta}, \mathbf{y})$ . We call the former one prior correlation matrix, denoted by  $\mathbf{R}_{prior}(\boldsymbol{\theta})$  and the later one posterior correlation matrix, denoted by  $\mathbf{R}_{post}(\boldsymbol{\theta})$ . We evaluate those correlation matrices at  $\boldsymbol{\theta}^*$ . Note that the correlation matrices are rarely fully evaluated and stored in order to avoid computational burden as they are dense and large. We will use either  $\mathbf{R}_{post} = \mathbf{R}_{post}(\boldsymbol{\theta}^*)$  or  $\mathbf{R}_{prior} = \mathbf{R}_{prior}(\boldsymbol{\theta}^*)$  to construct the groups. The correlation matrix for the linear predictors is central in our proposal for the definition of the groups we discuss the implications from each case.

The manually constructed groups are often based on prior knowledge and some interesting effects of  $\mathbf{f}$ . To imitate this process, we can compute the correlation matrix from a submatrix of  $\mathbf{P}_f(\boldsymbol{\theta})$ . The submatrix contains those interesting effects of  $\mathbf{f}$ . The correlation matrix,  $\mathbf{R}_{prior}$ , derived from the submatrix of the precision matrix is a conditional correlation matrix conditioning on those unselected effects. When we are unknowledgeable about our models, we recommend using  $\mathbf{R}_{post}$  to construct groups because data can help us determine the importance of each component.

With a correlation matrix  $\mathbf{R}$ , it is natural to choose  $I_i$  by including a fixed number of points that are most correlated to  $\eta_i$  into the group. This approach is problematic because many linear predictors are frequently identically correlated to  $\eta_i$ . It is more reasonable to include all the points identically correlated to  $\eta_i$  into  $I_i$  if one of them is included. We can define a level set to be all the points with the same absolute correlation to  $\eta_i$ . Then the size of the group is chosen based on the number of level sets,  $m$ , considered. More dependency between the training set and the testing point will be removed if we set higher  $m$ . In general, we recommend a small number of level sets when  $\mathbf{R}_{post}$  is used, like  $m = 3$ , since the group size will be too large if  $m$  is chosen to be high. As an example, in the last application of Section 5,  $m = 3$  creates a group with size of 20.

The automatic group construction process is summarized as follows. We set up the construction by choosing the number of the level sets,  $m$ , and which correlation matrix to use. Then, for each  $i$ , we can have  $m$  level sets associated with  $m$  largest absolute correlation to  $\eta_i$ . Finally, the union of those level sets is  $I_i$ .

We use some examples to demonstrate the group construction process using  $\mathbf{R}_{prior}$ . We will see that the automatically constructed groups are similar to the manually constructed groups and many level sets contain multiple members. The group construction process using  $\mathbf{R}_{post}$  is the same as using  $\mathbf{R}_{prior}$  but the resulting groups are affected by  $\mathbf{y}$ . We will show the groups constructed by  $\mathbf{R}_{post}$  in Section 5.

**Example** (Nested multilevel model). Assume we record students' grades  $\mathbf{y}$  and their self-rating  $\mathbf{x}$ . A student is from a class; A class is in a school; A school is in a region. We could model this data by an LGM,

$$\begin{aligned} \eta_i &= \mu + c_{j_c(i)} + s_{j_s(i)} + r_{j_r(i)} + \beta x_i, \\ \mathbf{c}, \mathbf{s}, \mathbf{r}, \beta, \mu | \boldsymbol{\theta} &\sim N(0, \mathbf{P}_f(\boldsymbol{\theta})). \end{aligned} \quad (7)$$

In model (7),  $j_c(i)$ ,  $j_s(i)$  and  $j_r(i)$  map  $i$  to student  $i$ 's class, school, and region index.  $\mathbf{P}_f(\boldsymbol{\theta})$  is a diagonal matrix with  $\boldsymbol{\theta} = \{\tau_r, \tau_s, \tau_c, \tau_\beta, \tau_\mu\}$  and  $\mathbf{P}_f(\boldsymbol{\theta}) = \text{diag}(\tau_r, \tau_r, \tau_s, \tau_s, \tau_s, \tau_c, \tau_c, \tau_c, \tau_c, \tau_c, \tau_c, \tau_\beta, \tau_\mu)$  which corresponds 2 regions, 2 schools in each region, and 2 classes in each school. For example, in Figure 1,  $j_c(12) = 6$ ,  $j_s(12) = 3$ ,  $j_r(12) = 2$ .

For simplicity of notation, we assume  $\theta^* = \{1, 1, 1, 1, 1\}$ . Then the unconditional correlation for  $\eta_i$  and  $\eta_j$  and the correlation conditioning on  $\mu$  and  $\beta$  are

$$\text{corr}(\eta_i, \eta_j) = \frac{\mathbb{1}_{j_c(i)=j_c(j)} + \mathbb{1}_{j_s(i)=j_s(j)} + \mathbb{1}_{j_r(i)=j_r(j)} + 1 + x_i x_j}{\sqrt{(4 + x_i^2)(4 + x_j^2)}},$$

$$\text{corr}(\eta_i, \eta_j | \mu, \beta) = \frac{\mathbb{1}_{j_c(i)=j_c(j)} + \mathbb{1}_{j_s(i)=j_s(j)} + \mathbb{1}_{j_r(i)=j_r(j)}}{3},$$

where  $\mathbb{1}_A$  is 1 if  $A$  is true and 0 otherwise. With the unconditional correlation, the groups reflect the correlation due to  $x_i$  and  $x_j$ . In practice, the groups may not be desirable because we usually assume  $\mathbf{x}$  are sampled randomly without structure.

With the conditional correlation, we have four level sets for each  $i$  which associate with absolute correlation equal to 0,  $\frac{1}{3}$ ,  $\frac{2}{3}$  and 1.  $I_i$  includes all students from the  $i$ th student's class when  $m = 1$ ;  $I_i$  includes all students from the  $i$ th student's school when  $m = 2$ ;  $I_i$  includes all students from the  $i$ th student's region when  $m = 3$ ;  $I_i$  includes all the data when  $m = 4$ . Groups produced by each number of level sets have a good interpretation in the example. For  $m = 1$ , the implied prediction task is predicting a student's grade in an unobserved class of an observed school; for  $m = 2$ , it is predicting a student's grade in an unobserved school of an observed region; for  $m = 3$ , it is predicting a student's grade in an unobserved region; for  $m = 4$ , we exclude all the data, which is a prior prediction; the implied prediction task of LOOCV is predicting a student's grade from an observed class. An automatically constructed group using  $\text{corr}(\eta_i, \eta_j | \mu, \beta)$  is shown in Figure 1 for  $i = 12$  with  $m = 2$ , which is  $I_{12} = \{12, 13, 14, 15, 10, 11\}$ .

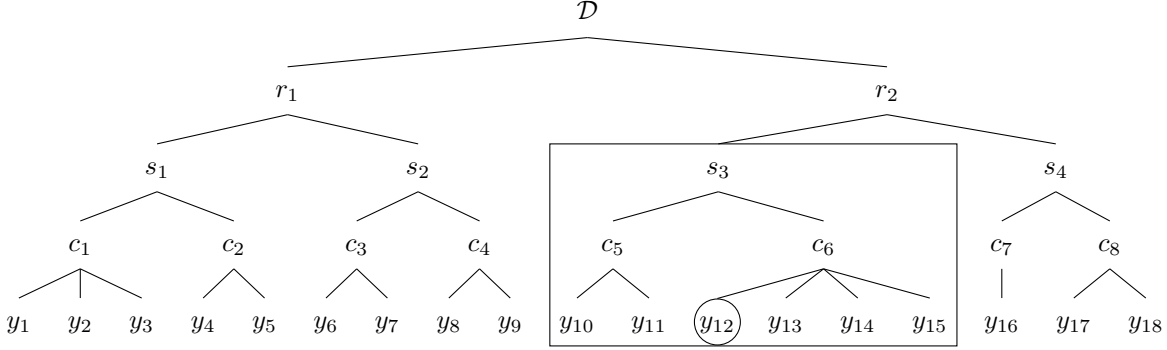


Figure 1: An automatically constructed group for nested multilevel model

We can also get reasonable groups through the spatial correlation when we have a spatial effect in the model.

**Example (Spatial Model).** Assume each data point is recorded with a spatial location  $s_i$ . The latent linear predictor can be specified by

$$\eta_i = \mu + f_{s_i}.$$

$f_s$  is often modeled by a Gaussian field with zero mean and an isotropic spatial correlation. Using the correlation derived from the spatial effects,  $I_i$  includes data within a circle centered by the testing point with a radius determined by  $m$ . By choosing  $m$  such that  $\text{var}(\eta_i | \eta_{-I}) \approx \text{var}(\eta_i)$ , the implied prediction task is predicting a data point from a remote area or a data point from a replicate of the Gaussian process. Figure 2 shows an automatically constructed group with  $m = 5$  with the solid point as the testing point. In the figure, the data in the circle are the group to be removed from the training set, and the group size is 6.

In the examples, the interesting model components for group construction are clear. However, in practice, we can encounter models with multiple important model components in the sense that they could be potentially included for group construction, like the last example in section 5. In this case, we recommend using  $R_{\text{post}}$  with small  $m$  if we can not decide which components are more important.

## 4 Approximation of Leave-group-out Cross-Validation

This section discusses how to approximate  $\pi(Y_i | \mathbf{y}_{-I_i})$ . The results are straightforward but great care is needed to make all the corner cases numerically stable. This new approach is more accurate and stable than the one published in [12] for LOOCV.

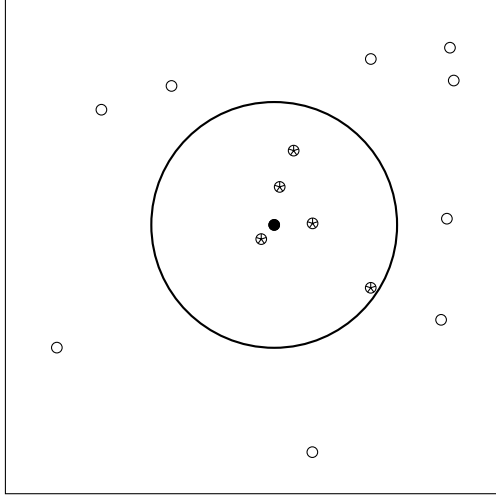


Figure 2: An automatically constructed group for a spatial model

We start by writing  $\pi(Y_i|\mathbf{y}_{-I_i})$  as a nested integral,

$$\pi(Y_i|\mathbf{y}_{-I_i}) = \int_{\boldsymbol{\theta}} \pi(Y_i|\boldsymbol{\theta}, \mathbf{y}_{-I_i}) \pi(\boldsymbol{\theta}|\mathbf{y}_{-I_i}) d\boldsymbol{\theta} \quad (8)$$

$$\pi(Y_i|\boldsymbol{\theta}, \mathbf{y}_{-I_i}) = \int \pi(Y_i|\eta_i, \boldsymbol{\theta}) \pi(\eta_i|\boldsymbol{\theta}, \mathbf{y}_{-I_i}) d\eta_i. \quad (9)$$

The integral (8) is computed by the numerical integration [12], and the integral (9) is computed by Gauss-Hermite quadratures [22] as  $\pi(\eta_i|\boldsymbol{\theta}, \mathbf{y}_{-I_i})$  will be approximated by a Gaussian distribution. The key to the accuracy of (9) is that the likelihood,  $\pi(Y_i|\eta_i, \boldsymbol{\theta})$ , is exact such that small approximation errors of  $\pi(\eta_i|\boldsymbol{\theta}, \mathbf{y}_{-I_i})$  diminish due to the integration. The accuracy of (8) relies on the accuracy of (9) and the assumption that the removal of  $\mathbf{y}_{I_i}$  does not have drastic impact on  $\pi(\boldsymbol{\theta}|\mathbf{y})$ .

The computation of the nested integrals boils down to the computation of  $\pi(\eta_i|\boldsymbol{\theta}, \mathbf{y}_{-I_i})$  and  $\pi(\boldsymbol{\theta}|\mathbf{y}_{-I_i})$ . We will approximate  $\pi(\eta_i|\boldsymbol{\theta}, \mathbf{y}_{-I_i})$  by a Gaussian based on (5), denoted by  $\pi_G(\eta_i|\boldsymbol{\theta}, \mathbf{y}_{-I_i})$ , and  $\pi(\boldsymbol{\theta}|\mathbf{y}_{-I_i})$  by correcting  $\pi(\boldsymbol{\theta}|\mathbf{y})$ . We further improve the mean of  $\pi_G(\eta_i|\boldsymbol{\theta}, \mathbf{y}_{-I_i})$  using variational Bayes [20] in the implementation. In this section, we focus on the explanation of computing  $\pi_G(\eta_i|\boldsymbol{\theta}, \mathbf{y}_{-I_i})$  and  $\pi(\boldsymbol{\theta}|\mathbf{y}_{-I_i})$ .

### Compute $\pi_G(\eta_i|\boldsymbol{\theta}, \mathbf{y}_{-I_i})$

The mean and variance of  $\pi_G(\eta_i|\boldsymbol{\theta}, \mathbf{y}_{-I_i})$  can be obtained by

$$\begin{aligned} \mu_{\eta_i}(\boldsymbol{\theta}, \mathbf{y}_{-I_i}) &= \mathbf{A}_i \boldsymbol{\mu}_f(\boldsymbol{\theta}, \mathbf{y}_{-I_i}), \\ \sigma_{\eta_i}^2(\boldsymbol{\theta}, \mathbf{y}_{-I_i}) &= \mathbf{A}_i \mathbf{Q}_f^{-1}(\boldsymbol{\theta}, \mathbf{y}_{-I_i}) \mathbf{A}_i^T. \end{aligned} \quad (10)$$

The computation of  $\pi_G(\mathbf{f}|\boldsymbol{\theta}, \mathbf{y}_{-I_i})$  requires the mode of  $\pi(\mathbf{f}|\boldsymbol{\theta}, \mathbf{y}_{-I_i})$  for each  $i$  at each configuration of  $\boldsymbol{\theta}$ , which is computationally expensive. With (5), we use an approximation to avoid the optimization step,

$$\mathbf{Q}_f(\boldsymbol{\theta}, \mathbf{y}_{-I_i}) \approx \tilde{\mathbf{Q}}_f(\boldsymbol{\theta}, \mathbf{y}_{-I_i}) = \mathbf{Q}_f(\boldsymbol{\theta}, \mathbf{y}) - \mathbf{A}_{I_i}^T \mathbf{C}_{I_i}(\boldsymbol{\theta}, \mathbf{y}) \mathbf{A}_{I_i}, \quad (11)$$

$$\boldsymbol{\mu}_f(\boldsymbol{\theta}, \mathbf{y}_{-I_i}) \approx \tilde{\boldsymbol{\mu}}_f(\boldsymbol{\theta}, \mathbf{y}_{-I_i}) = \tilde{\mathbf{Q}}_f(\boldsymbol{\theta}, \mathbf{y}_{-I_i})^{-1} (\mathbf{A}^T \mathbf{b}(\boldsymbol{\theta}, \mathbf{y}) - \mathbf{A}_{I_i}^T \mathbf{b}_{I_i}(\boldsymbol{\theta}, \mathbf{y})), \quad (12)$$

where  $\mathbf{A}_{I_i}$  is a submatrix of  $\mathbf{A}$  formed by rows of  $\mathbf{A}$ ,  $\mathbf{b}_{I_i}(\boldsymbol{\theta}, \mathbf{y})$  is a subvector of  $\mathbf{b}(\boldsymbol{\theta}, \mathbf{y})$ , and  $\mathbf{C}_{I_i}(\boldsymbol{\theta}, \mathbf{y})$  is a principal submatrix of  $\mathbf{C}(\boldsymbol{\theta}, \mathbf{y})$ . (11) and (12) are moments of the Gaussian approximation of  $\pi(\mathbf{f}|\boldsymbol{\theta}, \mathbf{y}_{-I_i})$  on the mode of  $\pi(\mathbf{f}|\boldsymbol{\theta}, \mathbf{y})$ . Hence, when the posterior is Gaussian, the approximation is exact. It seems easy to obtain the moments using (10), but the decomposition of  $\tilde{\mathbf{Q}}_f(\boldsymbol{\theta}, \mathbf{y}_{-I_i})$  is too expensive. To avoid the decomposition of  $\tilde{\mathbf{Q}}_f(\boldsymbol{\theta}, \mathbf{y}_{-I_i})$ , we use the linear relation  $\boldsymbol{\eta}_{I_i} = \mathbf{A}_{I_i} \mathbf{f}$  to map all the computation on  $\mathbf{f}$  to  $\boldsymbol{\eta}_{I_i}$ . We compute  $\boldsymbol{\Sigma}_{\boldsymbol{\eta}_{I_i}}(\boldsymbol{\theta}, \mathbf{y}_{-I_i})$  and  $\boldsymbol{\mu}_{\boldsymbol{\eta}_{I_i}}(\boldsymbol{\theta}, \mathbf{y}_{-I_i})$  through  $\boldsymbol{\Sigma}_{\boldsymbol{\eta}_{I_i}}(\boldsymbol{\theta}, \mathbf{y})$  and  $\boldsymbol{\mu}_{\boldsymbol{\eta}_{I_i}}(\boldsymbol{\theta}, \mathbf{y})$  as shown in Appendix A with a low rank representation, where  $\boldsymbol{\Sigma}_{\boldsymbol{\eta}_{I_i}}(\boldsymbol{\theta}, \mathbf{y})$  is the posterior covariance matrix of  $\boldsymbol{\eta}_{I_i}$  and  $\boldsymbol{\Sigma}_{\boldsymbol{\eta}_{I_i}}(\boldsymbol{\theta}, \mathbf{y}_{-I_i})$  is the covariance matrix of  $\boldsymbol{\eta}_{I_i}$  with  $\mathbf{y}_{I_i}$  left out. The computation of  $\boldsymbol{\Sigma}_{\boldsymbol{\eta}_{I_i}}(\boldsymbol{\theta}, \mathbf{y})$  is non-trivial especially when linear constraints are applied, which is demonstrated in Appendix B.

The approximation is more accurate when  $\pi(\eta_i|\boldsymbol{\theta}, \mathbf{y}_{-I_i})$  is close to Gaussian. The Gaussianity of  $\eta_i|\boldsymbol{\theta}, \mathbf{y}_{-I_i}$  comes from three sources. Firstly,  $\pi(\eta_i|\boldsymbol{\theta}, \mathbf{y}_{-I_i})$  is asymptotically Gaussian [23], which tends to be applicable when  $\eta_i$  is connected to large amount of data. Secondly,  $\pi(\eta_i|\boldsymbol{\theta}, \mathbf{y}_{-I_i})$  is dominated by the Gaussian prior, which happens when  $\eta_i$  is connected to few data. Thirdly, the likelihood is close to Gaussian.

### Approximate $\pi(\boldsymbol{\theta}|\mathbf{y}_{-I_i})$

To approximate  $\pi(\boldsymbol{\theta}|\mathbf{y}_{-I_i})$ , we consider the relation,

$$\pi(\boldsymbol{\theta}|\mathbf{y}_{-I_i}) \propto \frac{\pi(\boldsymbol{\theta}|\mathbf{y})}{\pi(\mathbf{y}_{I_i}|\boldsymbol{\theta}, \mathbf{y}_{-I_i})},$$

where we can approximate  $\pi(\boldsymbol{\theta}|\mathbf{y})$  at some configurations [12]. We need to compute  $\pi(\mathbf{y}_{I_i}|\boldsymbol{\theta}, \mathbf{y}_{-I_i})$ , which is

$$\pi(\mathbf{y}_{I_i}|\boldsymbol{\theta}, \mathbf{y}_{-I_i}) \approx \int \pi(\mathbf{y}_{I_i}|\boldsymbol{\eta}_{I_i}, \boldsymbol{\theta}) \pi_G(\boldsymbol{\eta}_{I_i}|\boldsymbol{\theta}, \mathbf{y}_{-I_i}) d\boldsymbol{\eta}_{I_i}.$$

A Laplace approximation approximates this integral,

$$\pi_{LA}(\mathbf{y}_{I_i}|\boldsymbol{\theta}, \mathbf{y}_{-I_i}) = \frac{\pi(\mathbf{y}_{I_i}|\boldsymbol{\eta}_{I_i}^*, \boldsymbol{\theta}) \pi_G(\boldsymbol{\eta}_{I_i}^*|\boldsymbol{\theta}, \mathbf{y}_{-I_i})}{\pi_G(\boldsymbol{\eta}_{I_i}^*|\boldsymbol{\theta}, \mathbf{y})}, \quad (13)$$

where  $\boldsymbol{\eta}_{I_i}^*$  is the mode of  $\pi_G(\boldsymbol{\eta}_{I_i}^*|\boldsymbol{\theta}, \mathbf{y})$ . Note that the correction of hyperparameter reuses  $\pi_G(\boldsymbol{\eta}_{I_i}|\boldsymbol{\theta}, \mathbf{y}_{-I_i})$  and  $\pi_G(\boldsymbol{\eta}_{I_i}^*|\boldsymbol{\theta}, \mathbf{y})$ .

### Approximate LGOCV Mean Square Error

With approximations of  $\pi(\boldsymbol{\theta}|\mathbf{y}_{-I_i})$  and  $\pi(\eta_i|\boldsymbol{\theta}, \mathbf{y}_{-I_i})$ , the computation of (1) is done. One can also compute the leave-group-out version of mean square loss as shown in (2). The expectation of the response is a simple integral,

$$E[Y_i|\mathbf{y}_{-I_i}] = \int_{\boldsymbol{\theta}} \int_{\eta_i} E[Y_i|\eta_i, \boldsymbol{\theta}] \pi(\eta_i|\boldsymbol{\theta}, \mathbf{y}_{-I_i}) \pi(\boldsymbol{\theta}|\mathbf{y}_{-I_i}) d\eta_i d\boldsymbol{\theta},$$

where the model gives  $E[Y_i|\eta_i, \boldsymbol{\theta}]$ . Other loss and utility functions can be achieved similarly.

## 5 Simulations and Applications

This section provides a simulated example and three real data applications. We start with a simulated example to verify the accuracy of the approximation in a multilevel model with different responses. We continue with a time series forecasting example to compare the results of LGOCV with automatically constructed groups and LFOCV. Then, we fit a model for disease mapping to compare groups constructed by different strategies. In the end, we apply our method to a model with complex structures on a large data set [24].

### Simulated Multilevel Model with Various Responses

This simulated example intends to show the accuracy of the approximation compared with MCMC. We consider a multilevel model [2],

$$\begin{aligned} y_i|\eta_i, \boldsymbol{\theta} &\sim \text{Likelihood}(\eta_i, \boldsymbol{\theta}), \\ \eta_i &= \mu + s_{j_s(i)}, \\ \boldsymbol{s}, \mu|\boldsymbol{\theta} &\sim N(0, \mathbf{P}_f(\boldsymbol{\theta})), \end{aligned} \quad (14)$$

which is a model describing observations sampled from different groups. In this model,  $\mathbf{P}_f(\boldsymbol{\theta})$  is a diagonal matrix similar to  $\mathbf{P}_f(\boldsymbol{\theta})$  in (7). We set the prior precision of the intercept  $\tau_\mu = 10^{-4}$  and assign a normal prior with mean 0 and precision  $10^{-4}$  to  $\log \tau_s$ . We will consider three cases where  $y_i$  has different likelihoods. For a Gaussian response, the precision of the likelihood is fixed to be 1. For a binomial response, we set the number of trials to be 20 and use a logit link. For an exponential response, we use a log link. There are natural groups in this model, which are used for LGOCV. This is a computationally hard case since the testing point can be only predicted by the intercept after removing the group, which means the removal has a large impact on the posterior.

We simulate data according to the specified model with 10 groups and 10 data points in each group. As a reference, the MCMC runs  $10^8$  iterations, which makes the Monte Carlo errors negligible. Large size of MCMC samples is

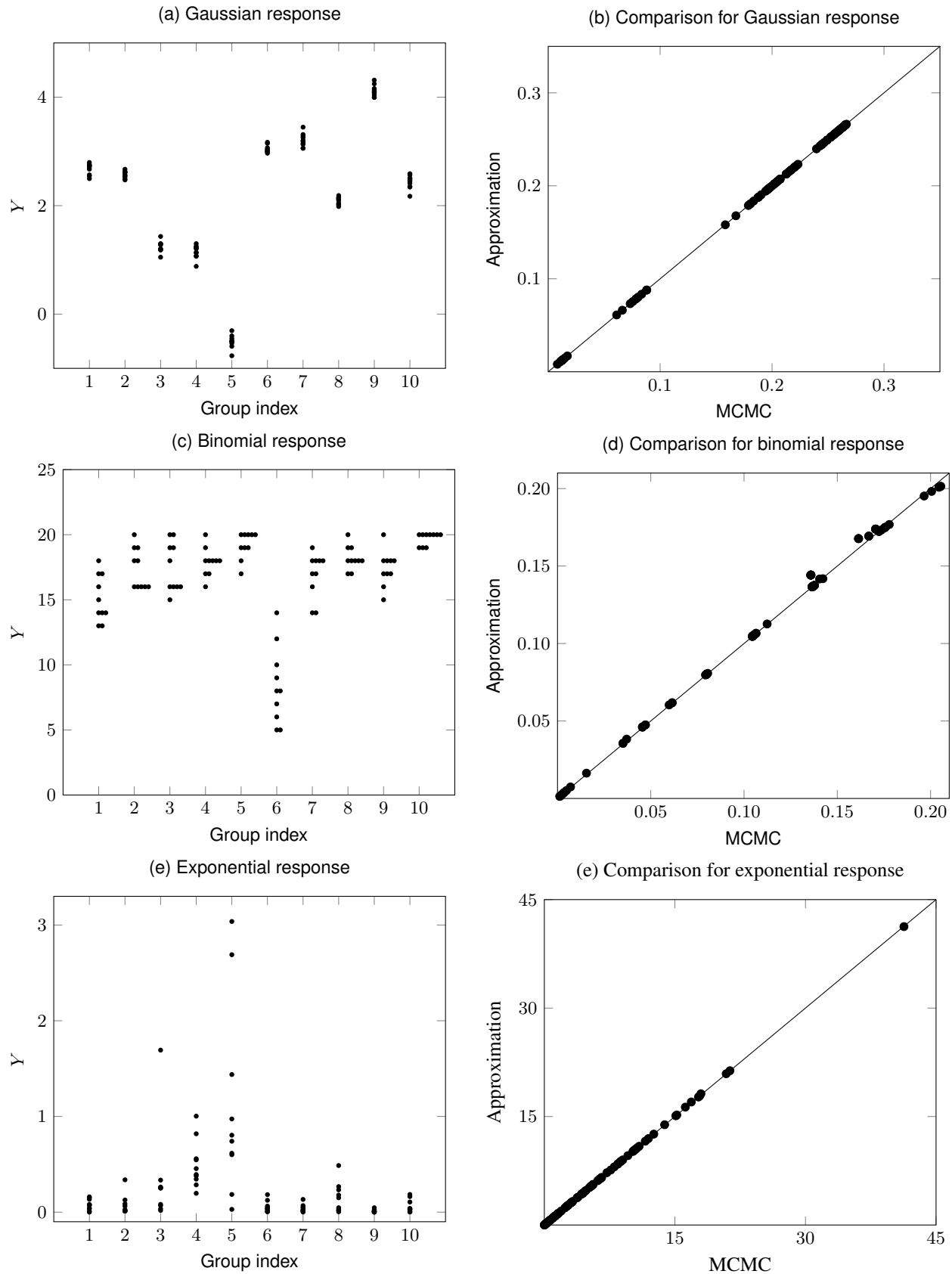


Figure 3: Our approximations compared with MCMC

required because the predictive distributions are influenced by the tails of  $\pi(\eta_i|\boldsymbol{\theta}, \mathbf{y}_{-I_i})$ . In Figure 3, (a), (c), and (d) show the data against its group index, which present a clear group structure; (b), (d), and (e) show the comparison of  $\pi(Y_i = y_i|\mathbf{y}_{-I_i})$  obtained from the approximations and MCMC. We use Rstan [25] to do MCMC.

This example shows that the approximations are highly accurate. When the response is Gaussian, the approximation almost equals the MCMC results, where the difference is due to MCMC sampling errors while our approach is exact up to numerical integration for this case. Also, under both non-Gaussian cases, the results are close to the long-run MCMC results.

### Earthquake Forecasting

In this example, we will show that the automatic LGOCV can measure the predictive performance of a time-series model. We fit a time series model on a data set recording the number of yearly major earthquakes from 1900 to 2006 in the world [26]. The model is:

$$\begin{aligned} y_i|\eta_i, \boldsymbol{\theta} &\sim \text{Poisson}(\exp(\eta_i)) \\ \eta_i &= \mu + u_t \end{aligned}$$

where  $u_t$  is modelled by an AR(1) model,  $\boldsymbol{\theta} = (\rho, \tau)$ ,  $\rho$  is the correlation in the AR(1) and  $\tau$  is the marginal precision of the AR(1). The priors are default priors in R-INLA. The left panel of Figure 5 exhibits the data and quantiles of  $\pi(e^{\eta_i}|\mathbf{y})$ .

Our potential prediction tasks are one-step forward forecasting, two steps forward forecasting, and three steps forward forecasting. Suitable manually defined groups for each task are demonstrated by Figure 4, where data points in the circles are the testing points and data points in the squares are groups. To make the training set similar to the observed data set, the first 50 data points are always in the training set, and they will not serve as testing points. We use the mean log predictive density as our utility function. We call the resulting predictive measurements LFOCV1, LFOCV2, and LFOCV3. We also compute LOOCV and the automatic LGOCV with the posterior correlation matrix and the number of level sets equal to 2. Most of the groups include data points one year before and after the testing point. The right panel of Figure 5 compares predictive measurements for the model. We can see that LOOCV is too optimistic if the prediction task is forecasting. Our automatically constructed LGOCV is close to LFOCV2, which can measure forecasting performance.

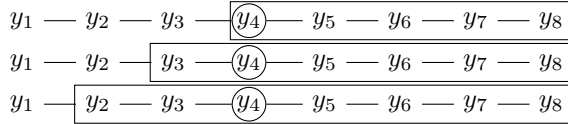


Figure 4: Manual groups for earthquake forecasting

### Disease Mapping

In this example, we will present groups constructed by different automatic group construction strategies on German maps. We will see the differences between those groups, and get an idea to choose a proper group construction strategy. We fit a model for disease mapping based on a data set describing cancer incidence with locations [27, 28, 29]. The data are incidence cases of oral cavity cancer in Germany, 1986-1990 [29]. The response  $y_i$  is the number of cases during the five years in area  $i$ . The number of cases in region  $i$  also depends on the population in that region and their age distribution. The expected number of cases of the disease in region  $i$  is calculated based on the age distribution and population such that  $\sum_i y_i = \sum_i E_i$ , where  $E_i$  is the expected counts. The covariate  $x_i$  is a measure for tobacco consumption in area  $i$ .

We fit the following model on the data set:

$$\begin{aligned} y_i|\eta_i, \boldsymbol{\theta} &\sim \text{Poisson}(E_i \exp(\eta_i)) \\ \eta_i &= \mu + f_{rw}(x_i) + u_i + v_i, \end{aligned} \tag{15}$$

where  $\mu$  is an intercept,  $u$  is a spatially structured component,  $v$  is an unstructured component [27, 30], and  $f_{rw}$  is an intrinsic second-order random-walk model of the covariate  $x_i$  [21].

In Figure 6, we display groups produced by different automatic group construction strategies. The testing point is measured from the black region, and the data in the group are measured from the grey regions. Groups in the first

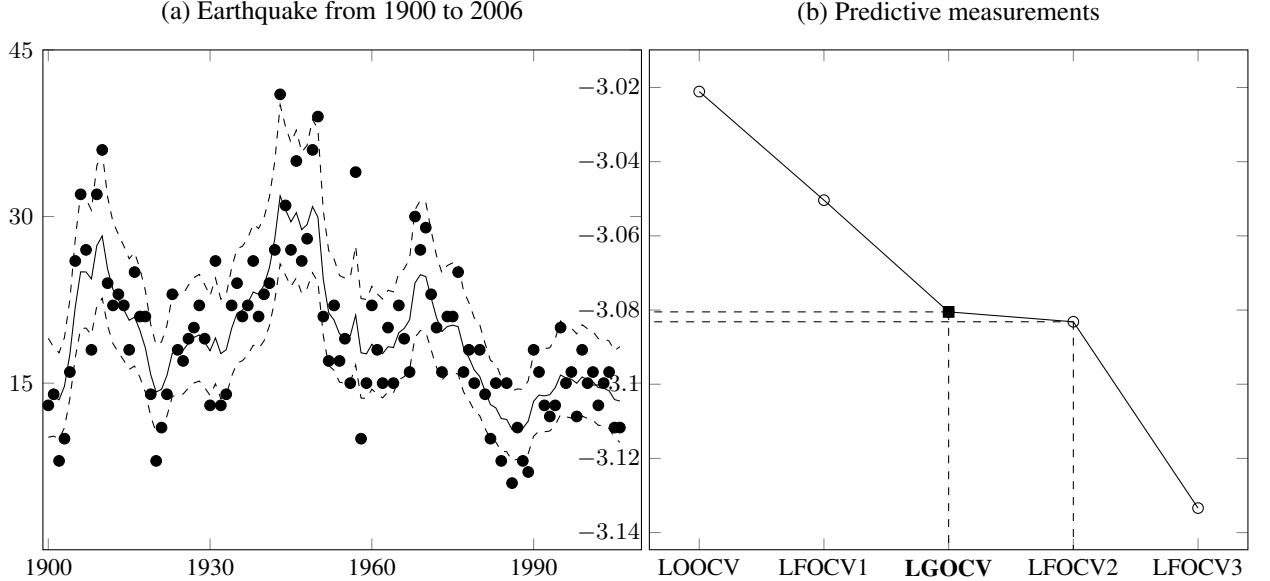


Figure 5: Automatic LGOCV compared with LFOCV

column are constructed by  $R_{prior}$ ; Groups in the second column are constructed by  $R_{prior}$  with only spatial effects; And groups in the third columns are constructed by  $R_{post}$ . The groups constructed by  $R_{prior}$  has weak spatial pattern because the group construction also uses correlation due to tobacco consumption. The groups constructed by  $R_{prior}$  with only spatial effects have strong spatial patterns as expected. The groups constructed by  $R_{post}$  exhibit strong spatial patterns in nearly all cases, but there are also a few non-spatial patterns in the groups because it takes all the model components into consideration: the fixed and random effects, priors and the response variable. The spatial pattern in the posterior groups may provide evidence to include the spatial effects in the model since data do not destroy the spatial pattern in the correlation. In practice, the manually defined groups are more similar to the one produced by  $R_{prior}$  with selected effects. The groups produced by  $R_{post}$  are more balanced with different model components. We do not recommend using the groups produced by  $R_{prior}$  without conditioning since the covariates often affect the group construction substantially while we usually assume covariates are sampled independently.

### Dengue Risk in Brazil

We will present an application of the automatic LGOCV to show the usefulness of the method in a real-world study with a complex model structure and large sample size. The variable selection process in [24] will be repeated using the automatic LGOCV with the number of level sets equal to 3. The model is aimed to quantify the non-linear and delayed effects of extreme hydrometeorological hazards on dengue risk by the level of urbanization in Brazil. The sample size of this dataset is 127,224, which records 12,895,293 dengue cases. The responses in the model are monthly notified dengue cases for each of 558 microregions of Brazil between January 2001 and December 2019. The data is associated with month, year, microregion, and state. The candidate covariates in this study are the monthly mean of daily minimum temperature ( $T_{min}$ ), monthly mean of daily maximum temperature ( $T_{max}$ ), self-calibrated Palmer drought severity index (PDSI), level of urbanization ( $u$ ), level of urbanization centered at high urbanized ( $u_1$ ), level of urbanization centered at intermediate urbanized ( $u_2$ ), level of urbanization centered at more rural level ( $u_3$ ), access to water supply service ( $w$ ), access to water supply service centered at high-frequency shortages ( $w_1$ ), access to water supply service centered at intermediate shortage ( $w_2$ ) and access to water supply service centered at low-frequency shortages ( $w_3$ ). Information about the preprocessing of those covariates can be found in [31]. The likelihood of the model is chosen to be negative binomial to account for overdispersion. The latent field consists of a temporal component describing a state-specific seasonality using a cyclic first difference prior distribution and a spatial component describing year-specific spatially unstructured and structured random effects using a modified Besag-York-Mollie (BYM2) model with a scaled spatial component [32]. The temporal component has replications for each state and the spatial component has replications for each year. We can express it using the formula,

$$\begin{aligned}
 y \sim & 1 + \text{covariates} \\
 & + f(\text{month, model} = "rw1", \text{replicates} = \text{stat}, \text{cyclic} = \text{TRUE}) \\
 & + f(\text{microregion, model} = "bym2", \text{replicates} = \text{year}).
 \end{aligned}$$

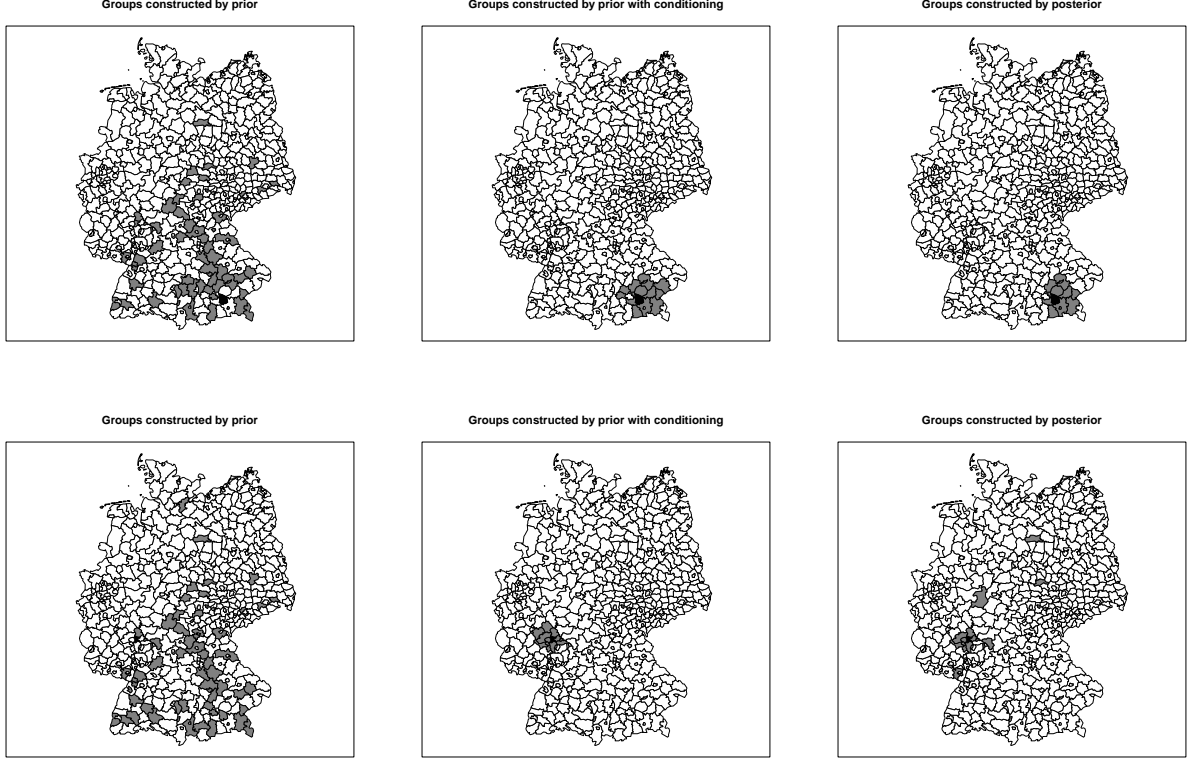


Figure 6: Groups by different automatic construction strategies

In short, we write this model as

$$y \sim 1 + \text{covariates} + f_t + f_s.$$

The number of parameters contained in this model is 21,567 for the full model. The appendix of [24] and its repository [31] provide full details about the models and data.

The model has a temporal effect with spatial replicates, a spatial effect with temporal replicates, and many constraints. It is not easy to come out with manually defined groups for LGOCV or identify important effects to include using the prior as previous examples. Thus the automatic group construction using posterior correlation is particularly useful in this rather complex model setting.

The model selection results using DIC, LOOCV, and LGOCV are shown in Table 1. The candidate models are identical to those in [31], and the results are computed using R-INLA. The loss function is negative mean log predictive density. In the table, we find LOOCV and DIC hardly distinguish between the last 4 models while LGOCV provides more distinguishable readings. LGOCV chooses a model different from the choice of DIC and LOOCV. We conclude that the model chosen by LGOCV could be taken as the one with better predictive ability than the one chosen based on the other criteria.

Additionally, the group constructed by the automatic group construction using the posterior correlation matrix is interpretable. For a given testing point, the group consists of data points from the same year, the same location, and near months in most cases. Figure 7 shows the relative frequencies of the month included in the group given the testing points are records of a given month. From the graph, we may conclude that the summer data is more informative for prediction. Even when the testing point is recorded in November, the group tends to include data in summer.

## 6 Discussion

CV is a useful tool for model assessment, but the blind trust of LOOCV is prevalent in the statistical practice, although this issue has been well-noticed [3, 33]. One reason is the lack of helpful tools to guide practitioners to design proper CV strategies and compute the corresponding CV utility. In this paper, we provide LGOCV as a framework to design

Model	DIC	LOOCV	LGOCV
$y \sim 1 + f_1 + f_2$	3629	0.01508	0.08167
$y \sim 1 + T_{min} + f_t + f_s$	1578	0.00641	0.03002
$y \sim 1 + T_{max} + f_t + f_s$	2237	0.00925	0.04254
$y \sim 1 + PDSI + f_t + f_s$	2166	0.00926	0.06449
$y \sim 1 + PDSI + T_{min} + f_t + f_s$	169	0.00062	0.01679
$y \sim 1 + PDSI + T_{max} + f_t + f_s$	914	0.00384	0.02338
$y \sim 1 + PDSI + T_{min} + PDSI * u_1 + u + f_t + f_s$	38	0.00012	0*
$y \sim 1 + PDSI + T_{min} + PDSI * u_2 + u + f_t + f_s$	32	0.00013	0.00087
$y \sim 1 + PDSI + T_{min} + PDSI * u_3 + u + f_t + f_s$	2	0.00017	0.00155
$y \sim 1 + PDSI + T_{min} + PDSI * w_1 + w + f_t + f_s$	5	0.00001	0.00970
$y \sim 1 + PDSI + T_{min} + PDSI * w_2 + w + f_t + f_s$	2	0.00001	0.00796
$y \sim 1 + PDSI + T_{min} + PDSI * w_3 + w + f_t + f_s$	0*	0*	0.00779

Note: We offset DIC by 826905, LOOCV by 3.27225 and LOGOCV by 3.59521.

Table 1: Model selection results

proper CV and emphasize the importance of designing CV according to the prediction tasks. More importantly, we proposed an efficient approximation of the utility function and a sensible way to construct groups automatically for a large class of models. We hope these new tools for LGOCV can lead to improving statistical practice to focus more on better predictive performance measurement.

The automatic LGOCV should not be used if the modeler has a CV strategy tailored to their applications. However, having a better default CV strategy than LOOCV is a significant advantage. The automatic LGOCV is constructed by summarizing some good CV practices in structured models and our understanding of LGMs. As such, we believe that the automatic LGOCV is useful for real-world applications, and it is a good starting point to define a more suitable CV.

## A On the computation of $\Sigma_{\eta_{I_i}}(\theta, \mathbf{y}_{-I_i})$ and $\mu_{\eta_{I_i}}(\theta, \mathbf{y}_{-I_i})$

In this section, we let  $I_i$  be  $I$  and drop  $\theta$  to simplify the notation without losing generality. We have a random vector  $\eta_I | \mathbf{y} \sim N(\mu_{\eta_I}(\mathbf{y}), \Sigma_{\eta_I}(\mathbf{y}))$ , which is a posterior distribution with prior  $\eta_I | \mathbf{y}_{-I} \sim N(\mu_{\eta}(\mathbf{y}_{-I}), \Sigma_{\eta}(\mathbf{y}_{-I}))$  and likelihood  $\pi_G(\mathbf{y}_I | \eta_I) \propto \exp \left\{ -\frac{1}{2} \eta_I^T \mathbf{C}(\mathbf{y}_I) \eta_I + b(\mathbf{y}_I) \eta_I \right\}$ . Now, we need to use the posterior and the likelihood to obtain the prior.

If  $\Sigma_{\eta_I}(\mathbf{y})$  is full rank, we have  $\mathbf{Q}_{\eta_I}(\mathbf{y}) = \Sigma_{\eta}(\mathbf{y})^{-1}$  and  $\mathbf{b}_{\eta_I}(\mathbf{y}) = \mathbf{Q}_{\eta}(\mathbf{y}) \mu_{\eta}(\mathbf{y})$ . By conjugacy of Gaussian prior and Gaussian likelihood,  $\mathbf{Q}_{\eta_I}(\mathbf{y}_{-I}) = \mathbf{Q}_{\eta}(\mathbf{y}) - \mathbf{C}(\mathbf{y}_I)$  and  $\mathbf{b}_{\eta_I}(\mathbf{y}_{-I}) = \mathbf{Q}_{\eta}(\mathbf{y}) \mu_{\eta}(\mathbf{y}) - b(\mathbf{y}_I)$ . Then we have desired  $\mu_{\eta}(\mathbf{y}_{-I})$  and  $\Sigma_{\eta}(\mathbf{y}_{-I})$ .

If  $\Sigma_{\eta_I}(\mathbf{y})$  is singular, we let  $\eta | \mathbf{y} = \mathbf{Bz} | \mathbf{y}$ , where  $\mathbf{B} = \mathbf{V}\Lambda$  with  $\mathbf{V}$  containing eigenvectors corresponding to non-zero eigenvalues,  $\Lambda$  containing square root of non-zero eigenvalues on its diagonal, and  $\mathbf{z} | \mathbf{y} \sim N(\mu_{\mathbf{z}}(\mathbf{y}), \mathbf{I})$ , where  $\mathbf{I}$  is an identity matrix and  $\mathbf{B}\mu_{\mathbf{z}}(\mathbf{y}) = \mu_{\eta_I}(\mathbf{y})$ . By conjugacy, we have  $\mathbf{Q}_{\mathbf{z}}(\mathbf{y}_{-I}) = \mathbf{I} - \mathbf{B}^T \mathbf{C}(\mathbf{y}_I) \mathbf{B}$  and  $\mathbf{b}_{\mathbf{z}}(\mathbf{y}_{-I}) = \mu_{\mathbf{z}}(\mathbf{y}) - \mathbf{B}^T b(\mathbf{y}_I)$ . Then mean of  $\mathbf{z} | \mathbf{y}_{-I}$  solves  $\mathbf{Q}_{\mathbf{z}}(\mathbf{y}_{-I}) \mu_{\mathbf{z}}(\mathbf{y}_{-I}) = \mathbf{b}_{\mathbf{z}}(\mathbf{y}_{-I})$ . It is followed by  $\mu_{\eta}(\mathbf{y}_{-I}) = \mathbf{B}\mu_{\mathbf{z}}(\mathbf{y}_{-I})$  and  $\Sigma_{\eta}(\mathbf{y}_{-I}) = \mathbf{B}\Sigma_{\mathbf{z}}(\mathbf{y}_{-I})\mathbf{B}^T$ .

## B On the computation of $\Sigma_{\eta_{I_i}}(\theta, \mathbf{y})$ and $\mu_{\eta_{I_i}}(\theta, \mathbf{y})$ with Linear Constraints

We start by illustrating how to compute  $\Sigma_{\eta_{I_i}}(\theta, \mathbf{y})$  and  $\mu_{\eta_{I_i}}(\theta, \mathbf{y})$  without linear constraints, and we apply the linear constraints to the targets. The computation of  $\mu_{\eta_{I_i}}(\theta, \mathbf{y})$  is simple, and  $\mu_{\eta_{I_i}}(\theta, \mathbf{y}) = \mathbf{A}_{I_i} \mathbf{Q}_f(\theta, \mathbf{y})$ . However, we never store large dense matrix like  $\mathbf{Q}_f(\theta, \mathbf{y})^{-1}$ . Thus,  $\Sigma_{\eta_{I_i}}(\theta, \mathbf{y})$  cannot be obtained by using matrix multiplication  $\mathbf{A}_{I_i} \mathbf{Q}_f(\theta, \mathbf{y})^{-1} \mathbf{A}_{I_i}^T$ . Instead, we compute  $\Sigma_{\eta}(\theta, \mathbf{y})$  entry by entry and use the result to fill in entries of  $\Sigma_{\eta_{I_i}}(\theta, \mathbf{y})$ . We compute  $\Sigma_{\eta}(\theta, \mathbf{y})_{i,j}$  by solving  $\mathbf{Q}_f(\theta, \mathbf{y}) \mathbf{x} = \mathbf{A}_i$  and  $\Sigma_{\eta}(\theta, \mathbf{y})_{i,j} = \mathbf{A}_j \mathbf{x}$ . The computation is fast because  $\mathbf{A}$  and  $\mathbf{Q}_f(\theta, \mathbf{y})$  are sparse, and the factorization of  $\mathbf{Q}_f(\theta, \mathbf{y})$  is reused.

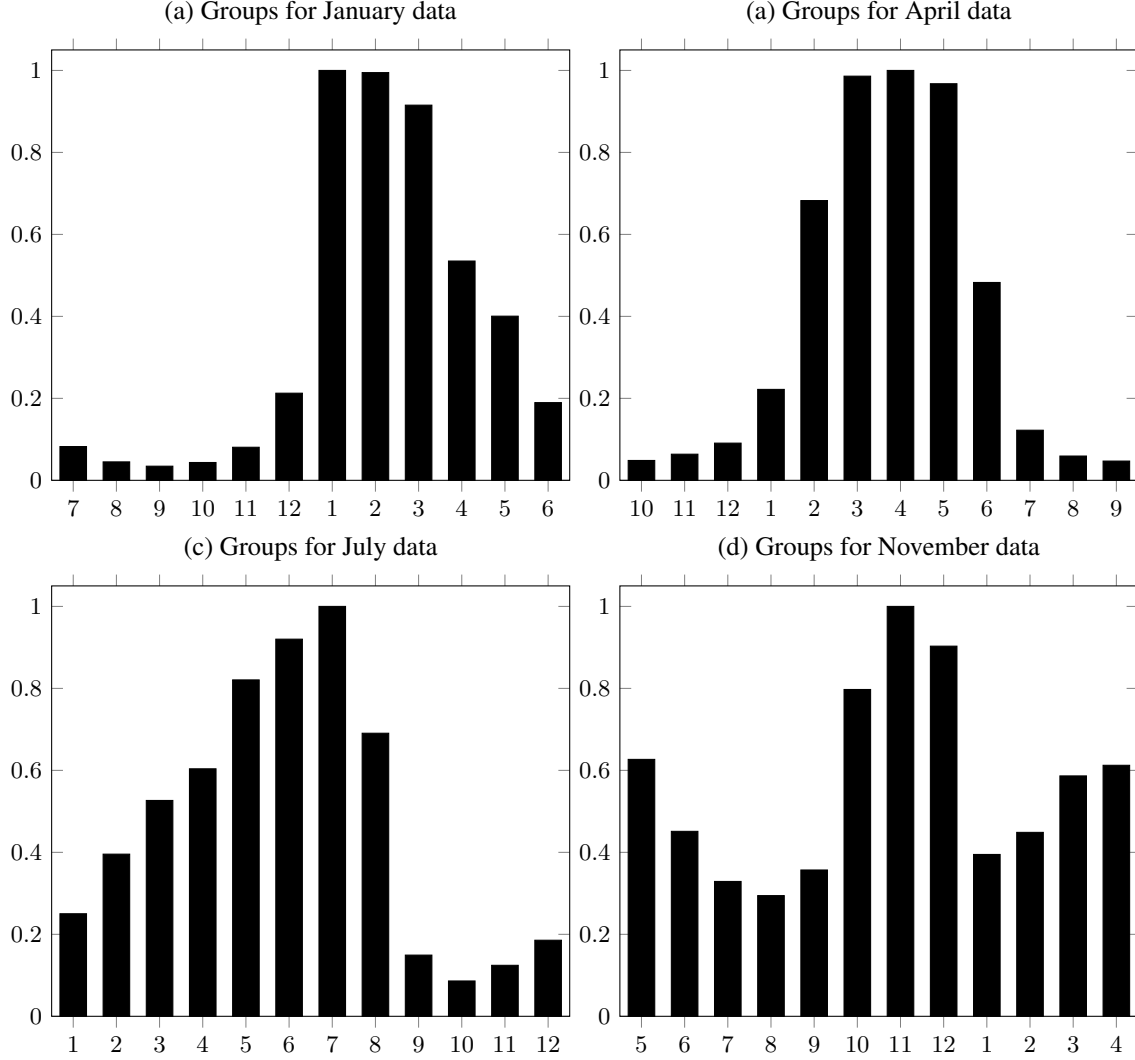


Figure 7: Groups for testing points from a given month

When linear constraints  $\mathcal{C}f = e$  are applied on  $f$ , we have

$$\begin{aligned}\Sigma_f(\theta, y)^* &= Q_f(\theta, y)^{-1} - Q_f(\theta, y)^{-1}\mathcal{C}^T(\mathcal{C}Q_f(\theta, y)^{-1}\mathcal{C}^T)^{-1}\mathcal{C}Q_f(\theta, y)^{-1}, \\ \mu_f(\theta, y)^* &= \mu_f(\theta, y) - Q_f(\theta, y)^{-1}\mathcal{C}^T(\mathcal{C}Q_f(\theta, y)^{-1}\mathcal{C}^T)^{-1}(\mathcal{C}\mu_f - e),\end{aligned}$$

where  $\Sigma_f(\theta, y)^*$  and  $\mu_f(\theta, y)^*$  are the mean and the covariance matrix after applying constraints [21]. Because  $\mu_f(\theta, y)^*$  is always stored, the computation of  $\mu_{\eta_{I_i}}(\theta, y)$  is simple. We need to propagate the effects of linear constraints to  $\Sigma_{\eta}(\theta, y)_{i,j}$ . This is achieved by computing [21]

$$\mathbf{x}^* = \mathbf{x} - Q_f(\theta, y)^{-1}\mathcal{C}^T(\mathcal{C}Q_f(\theta, y)^{-1}\mathcal{C}^T)^{-1}\mathcal{C}\mathbf{x},$$

where  $\mathbf{x}$  solves  $Q_f(\theta, y)\mathbf{x} = \mathbf{A}_i$ . Then

$$\Sigma_{\eta}(\theta, y)_{i,j}^* = \mathbf{A}_j \mathbf{x}^*,$$

where  $\Sigma_{\eta}(\theta, y)_{i,j}^*$  is the result of propagating the effects of linear constraints to  $\Sigma_{\eta}(\theta, y)_{i,j}$ .

## References

[1] Trevor Hastie, Robert Tibshirani, Jerome H Friedman, and Jerome H Friedman. *The elements of statistical learning: data mining, inference, and prediction*, volume 2. Springer, 2009.

- [2] Andrew Gelman, John B Carlin, Hal S Stern, and Donald B Rubin. *Bayesian data analysis*. Chapman and Hall/CRC, 1995.
- [3] David R Roberts, Volker Bahn, Simone Ciuti, Mark S Boyce, Jane Elith, Gurutzeta Guillera-Arroita, Severin Hauenstein, José J Lahoz-Monfort, Boris Schröder, Wilfried Thuiller, et al. Cross-validation strategies for data with temporal, spatial, hierarchical, or phylogenetic structure. *Ecography*, 40(8):913–929, 2017.
- [4] Sohrab Saeb, Luca Lonini, Arun Jayaraman, David C Mohr, and Konrad P Kording. The need to approximate the use-case in clinical machine learning. *Gigascience*, 6(5):gix019, 2017.
- [5] Leopoldo M Ruiz Maraggi, Larry W Lake, and Mark P Walsh. Using bayesian leave-one-out and leave-future-out cross-validation to evaluate the performance of rate-time models to forecast production of tight-oil wells. In *SPE/AAPG/SEG Unconventional Resources Technology Conference*. OnePetro, 2021.
- [6] Paul-Christian Bürkner, Jonah Gabry, and Aki Vehtari. Approximate leave-future-out cross-validation for bayesian time series models. *Journal of Statistical Computation and Simulation*, 90(14):2499–2523, 2020.
- [7] RJ Telford and HJB Birks. Evaluation of transfer functions in spatially structured environments. *Quaternary Science Reviews*, 28(13-14):1309–1316, 2009.
- [8] Prabir Burman, Edmond Chow, and Deborah Nolan. A cross-validatory method for dependent data. *Biometrika*, 81(2):351–358, 1994.
- [9] Arthur P Dempster, Nan M Laird, and Donald B Rubin. Maximum likelihood from incomplete data via the em algorithm. *Journal of the Royal Statistical Society: Series B (Methodological)*, 39(1):1–22, 1977.
- [10] Rebecca R Andridge and Roderick JA Little. A review of hot deck imputation for survey non-response. *International statistical review*, 78(1):40–64, 2010.
- [11] Michael L Stein. *Interpolation of spatial data: some theory for kriging*. Springer Science & Business Media, 2012.
- [12] Håvard Rue, Sara Martino, and Nicolas Chopin. Approximate bayesian inference for latent gaussian models by using integrated nested laplace approximations. *Journal of the royal statistical society: Series b (statistical methodology)*, 71(2):319–392, 2009.
- [13] Janet Van Niekerk, Elias Krainski, Denis Rustand, and Haavard Rue. A new avenue for bayesian inference with inla. *arXiv preprint arXiv:2204.06797*, 2022.
- [14] Aki Vehtari, Andrew Gelman, and Jonah Gabry. Practical bayesian model evaluation using leave-one-out cross-validation and waic. *Statistics and computing*, 27(5):1413–1432, 2017.
- [15] Soumya Ghosh, William T Stephenson, Tin D Nguyen, Sameer K Deshpande, and Tamara Broderick. Approximate cross-validation for structured models. *arXiv preprint arXiv:2006.12669*, 2020.
- [16] Assaf Rabinowicz and Saharon Rosset. Cross-validation for correlated data. *Journal of the American Statistical Association*, pages 1–14, 2020.
- [17] Tilmann Gneiting and Adrian E Raftery. Strictly proper scoring rules, prediction, and estimation. *Journal of the American statistical Association*, 102(477):359–378, 2007.
- [18] Daniel Commenges, Benoit Liquet, and Cécile Proust-Lima. Choice of prognostic estimators in joint models by estimating differences of expected conditional kullback–leibler risks. *Biometrics*, 68(2):380–387, 2012.
- [19] Håvard Rue, Andrea Riebler, Sigrunn H Sørbye, Janine B Illian, Daniel P Simpson, and Finn K Lindgren. Bayesian computing with inla: a review. *Annual Review of Statistics and Its Application*, 4:395–421, 2017.
- [20] Janet van Niekerk and Haavard Rue. Correcting the laplace method with variational bayes. *arXiv preprint arXiv:2111.12945*, 2021.
- [21] Havard Rue and Leonhard Held. *Gaussian Markov random fields: theory and applications*. Chapman and Hall/CRC, 2005.
- [22] Qing Liu and Donald A Pierce. A note on gauss—hermite quadrature. *Biometrika*, 81(3):624–629, 1994.
- [23] Andrew M Walker. On the asymptotic behaviour of posterior distributions. *Journal of the Royal Statistical Society: Series B (Methodological)*, 31(1):80–88, 1969.
- [24] Rachel Lowe, Sophie A Lee, Kathleen M O'Reilly, Oliver J Brady, Leonardo Bastos, Gabriel Carrasco-Escobar, Rafael de Castro Catão, Felipe J Colón-González, Christovam Barcellos, Marilia Sá Carvalho, et al. Combined effects of hydrometeorological hazards and urbanisation on dengue risk in brazil: a spatiotemporal modelling study. *The Lancet Planetary Health*, 5(4):e209–e219, 2021.
- [25] Stan Development Team. RStan: the R interface to Stan, 2022. R package version 2.21.5.

- [26] Jiahua Chen Shaoting Li and Pengfei Li. *MixtureInf: Inference for Finite Mixture Models*, 2016. R package version 1.1.
- [27] Julian Besag, Jeremy York, and Annie Mollié. Bayesian image restoration, with two applications in spatial statistics. *Annals of the institute of statistical mathematics*, 43(1):1–20, 1991.
- [28] Jonathan C Wakefield, NG Best, and L Waller. Bayesian approaches to disease mapping. *Spatial epidemiology: methods and applications*, pages 104–127, 2000.
- [29] Leonhard Held, Isabel Natário, Sarah Elaine Fenton, Håvard Rue, and Nikolaus Becker. Towards joint disease mapping. *Statistical methods in medical research*, 14(1):61–82, 2005.
- [30] Annie Mollié. Bayesian mapping of disease. *Markov chain Monte Carlo in practice*, 1:359–379, 1996.
- [31] Rachel Lowe. Data and R code to accompany ‘Combined effects of hydrometeorological hazards and urbanisation on dengue risk in Brazil: a spatiotemporal modelling study’, March 2021.
- [32] Andrea Riebler, Sigrunn H Sørbye, Daniel Simpson, and Håvard Rue. An intuitive bayesian spatial model for disease mapping that accounts for scaling. *Statistical methods in medical research*, 25(4):1145–1165, 2016.
- [33] Aki Vehtari, Daniel P Simpson, Yuling Yao, and Andrew Gelman. Limitations of “limitations of bayesian leave-one-out cross-validation for model selection”. *Computational Brain & Behavior*, 2(1):22–27, 2019.